J. Am. Soc. Mass Spectrom. (2018) 29:752–760
DOI: 10.1007/s13361-018-1902-5

RESEARCH ARTICLE

Resolution and Assignment of Differential Ion Mobility Spectra of Sarcosine and Isomers

Francis Berthias,[1] Belkis Maatoug,[1] Gary L. Glish,[2] Fathi Moussa,[3,4] Philippe Maitre[1]

[1]Laboratoire de Chimie Physique, Bâtiment 349, Université Paris-Sud, CNRS, Université Paris-Saclay, F-91405, Orsay, France
[2]Department of Chemistry, Caudill Laboratories, The University of North Carolina at Chapel Hill, Chapel Hill, NC 27599-3290, USA
[3]Université Paris-Sud, LETIAM, Lip(Sys)2, IUT d'Orsay, Plateau de Moulon, 91400, Orsay, France
[4]Biochemistry and Neuropediatric services, Hospital Group A. Trousseau-La Roche-Guyon, APHP, 75012, Paris, France

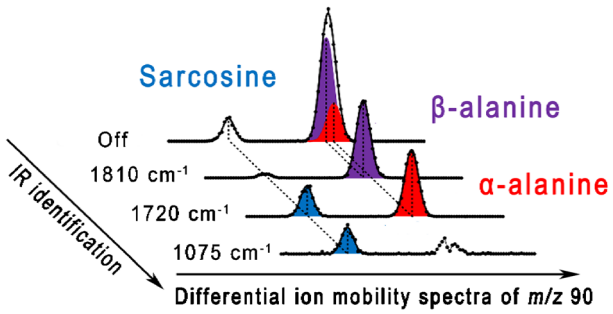

Abstract. Due to their central role in biochemical processes, fast separation and identification of amino acids (AA) is of importance in many areas of the biomedical field including the diagnosis and monitoring of inborn errors of metabolism and biomarker discovery. Due to the large number of AA together with their isomers and isobars, common methods of AA analysis are tedious and time-consuming because they include a chromatographic separation step requiring pre- or post-column derivatization. Here, we propose a rapid method of separation and identification of sarcosine, a biomarker candidate of prostate cancer, from isomers using differential ion mobility spectrometry (DIMS) interfaced with a tandem mass spectrometer (MS/MS) instrument. Baseline separation of protonated sarcosine from α- and β-alanine isomers can be easily achieved. Identification of DIMS peak is performed using an isomer-specific activation mode where DIMS- and mass-selected ions are irradiated at selected wavenumbers allowing for the specific fragmentation via an infrared multiple photon dissociation (IRMPD) process. Two orthogonal methods to MS/MS are thus added, where the MS/MS(IRMPD) is nothing but an isomer-specific multiple reaction monitoring (MRM) method. The identification relies on the comparison of DIMS-MS/MS(IRMPD) chromatograms recorded at different wavenumbers. Based on the comparison of IR spectra of the three isomers, it is shown that specific depletion of the two protonated α- and β-alanine can be achieved, thus allowing for clear identification of the sarcosine peak. It is also demonstrated that DIMS-MS/MS(IRMPD) spectra in the carboxylic C=O stretching region allow for the resolution of overlapping DIMS peaks.

Keywords: Tandem mass spectrometry, Ion mobility, Differential ion mobility, Infrared spectroscopy, Quantum chemical calculations, Amino acid, Sarcosine, Metabolomic

Received: 31 October 2017/Revised: 13 January 2018/Accepted: 18 January 2018/Published Online: 21 February 2018

Introduction

Due to their fundamental role in many biochemical processes, differential metabolomics profiling of common α-amino acids (AA) and their derivatives constitutes an unavoidable tool in many areas of biochemistry including the detection of inborn errors of metabolism and the discovery of biomarker candidates [1–6]. Due to the large number of AA, countless separation methods based on the charge and/or on hydrophobicity differences have been proposed for their metabolomics profiling. Liquid chromatographic (LC) methods with pre- or post-column derivatization to enhance the retention of the analytes and/or the sensitivity of detection are the most common methods for AA analysis [7]. However, while relatively free of interferences, these methods remain tedious and time-consuming. Recently, analysis of underivatized AA has

Electronic supplementary material The online version of this article (https://doi.org/10.1007/s13361-018-1902-5) contains supplementary material, which is available to authorized users.

Correspondence to: Philippe Maitre; *e-mail:* philippe.maitre@u–psud.fr

been performed using hydrophilic interaction liquid chromatography (HILIC) coupled to mass spectrometric detection (MS) [8]. Avoiding the derivatization step of AA may result in improved precision, absence of side reactions and reagent interferences, and shortened run time. Also, multiple reaction monitoring (MRM)-based protocols [9] have been proposed where tandem mass spectrometry (MS/MS) is coupled with efficient separation techniques such as gas chromatography and/or liquid chromatography [10], or capillary electrophoresis [11, 12], in order to resolve isobaric and/or isomeric species. Nevertheless, in the field of biomarker discovery and validation, fast and reproducible analytical methods of AA are still needed.

Ion mobility spectrometry (IMS) integrated to tandem mass spectrometry (IMS-MS/MS) represents an interesting alternative method not only in terms of running time but also as a derivatization-free technique [13]. Ion separation using IMS relies on their relative velocity in a buffer gas at nearly atmospheric pressure under the influence of an electric field. An interesting feature of ion mobility spectrometers is that they operate on time scale that is several orders of magnitude faster than gas or condensed phase chromatography. As a result, IMS instruments can be integrated to LC-MS/MS, thus offering two separation stages. A protocol based on a GC/LC-MS has been recently proposed for metabolomics and lipidomics [14]. IMS coupled with multiple ion monitoring has been shown to be powerful for regulatory LC-MS/MS bioanalysis of a therapeutic cyclic peptide in human plasma [15]. In addition, although gas and liquid chromatography separation conditions can be tailored for the separation of specific isomeric classes, IMS-MS/MS has been successfully applied to the resolution of isobars and isomers of small molecules [13]. For example, separation of 300 isomeric metabolites, within various classes of metabolites, has been achieved for human blood metabolomics profiling [16]. However, the separation and/or specific detection of some isomers exhibiting identical fragment ions such as sarcosine and α-alanine remain challenging because they are undistinguishable by using the MRM mode since their fragment ions are identical.

Our objective is to build on these achievements based on IMS-MS/MS. The idea is to further improve and accelerate the identification step using an infrared laser for the specific activation and fragmentation of isomers of interest. As recently reviewed [17], two classes of instruments can be distinguished depending whether ions are time- or space-separated. The latter has been chosen with differential ion mobility spectrometry (DIMS). The reason for this choice is that DIMS-selected ions can be continuously accumulated in an ion trap, which facilitates subsequent MS/MS sequences.

The performance of this novel approach is illustrated on the DIMS separation and IR identification of sarcosine, α-alanine, and β-alanine which are three isomers of $C_3H_7NO_2$. Sarcosine, an N-methyl derivative of glycine, has recently been identified as a differential metabolite across 262 clinical samples related to prostate cancer using liquid and gas chromatography coupled to mass spectrometry (LC-MS and GC-MS) [18]. While the role of sarcosine as a biomarker of prostate cancer is still a matter of debate, recent findings using ion exchange chromatography with Vis detection after post-column derivatization with ninhydrin show that sarcosine can upregulate the expression of some genes involved in cell cycle progression of metastatic models of prostate cancer [19]. Hence, fast and accurate method of sarcosine analysis may be a convenient tool for the elucidation of the physiopathological role of this AA.

Several attempts have been made for the separation of sarcosine and its isomers using time-separated-based IMS integrated with MS/MS methods [20–22]. It should be noted that a separation step is required prior MS/MS since protonated sarcosine and α-alanine are undistinguishable using MRM, since their fragment ions are identical. As part of a study for the assessment of electrospray ion, mobility approach for the detection and identification of organic molecules, 14 AA, including sarcosine and β-alanine, has been studied [21, 23]. It was shown in particular that sarcosine and β-alanine were well baseline resolved using N_2 as a drift gas. Separation of a simple standard mixture of α-alanine and sarcosine was investigated by another ion mobility technique [22]. While interesting preliminary results on identification of these compounds within a spiked urine sample were shown, the mobility spectra for α-alanine and sarcosine displayed multiple peaks apart from the main ones, which were not fully resolved. More recently, a better separation of a mixture of α-alanine and sarcosine has been achieved using a corona discharge ion mobility spectrometer [20]. Similar efforts to ascertain the potential of ion mobility mass spectrometry for the separation of amino acid isomers have been made in the case of leucine [24].

The aim of this study is to highlight that fast isomer separation and identification can be achieved by coupling DIMS and tandem mass spectrometry (MS/MS) integrating an isomer-specific activation mode. A systematic study of the dispersion plots shows that sarcosine can be easily separated from alanine isomers. Separation of α- and β-alanine, however, can only be achieved with the addition of a gas modifier, methanol, in the N_2 carrier gas. The principal novelty of the method proposed here is the isomer-specific fragmentation which is achieved by irradiating DIMS- and mass-selected ions at selected wavenumbers. This allows for the fragmentation of specific isomers through an infrared multiple photon dissociation (IRMPD) process. This is illustrated by DIMS-MS/MS(IRMPD) spectra where DIMS- and mass-selected ions were irradiated at fixed wavenumber selected for selective isomer fragmentation. Such DIMS spectra recorded at various wavelengths corresponding to IR signatures of different isomers show that overlapping peaks can be resolved and that isomer identification can be achieved.

Method

Sarcosine, α-alanine, and β-alanine were purchased from Sigma-Aldrich (St. Louis, MO, USA) and used without further purification. They were dissolved in a mixture of 10% acetic acidic methanol/water (50/50, *v*/*v*) at a final concentration of 100 μM. Similarly, mixture solutions were prepared with a 100-μM concentration of each amino acid. Positive ions corresponding to protonated amino acids are generated by electrospray, and the sample flow rate is set to 100 μL min^{-1}.

All the experiments were performed using an Esquire 3000+ quadrupole ion trap mass spectrometer (Bruker-Daltonics, Bremen, Germany) featuring an electrospray ionization (ESI) source. This instrument was modified in order to irradiate mass-selected ions within the ion trap [25], allowing for IR-specific activation of the ions which can be fragmented through an IR multiple photon dissociation (IRMPD) process [26]. The setup integrating differential ion mobility spectrometry is based on the one developed by Glish and coworkers [27]. The resulting DIMS-MS/MS(IRMPD) instrument allows for the DIMS-selected ions to be transmitted through the capillary to the quadrupole ion trap where they can be accumulated, mass-selected, and then subjected to multiple collisions with the He buffer gas or infrared-induced dissociation. The present DIMS-MS/MS(IRMPD) setup is very similar to that used for the characterization of monosaccharide complexes [28], except for the DIMS electronics and control program. A LabView program (v12.0.1f5, National Instrument) has been developed in order to control the radio frequency field and the data acquisition, which is synchronized with the Bruker acquisition software under chromatogram mode.

Briefly, the DIMS device has been designed in such a way to replace the spray shield of the Bruker Esquire. It is integrated between the ESI emitter and the capillary transfer. Positive ions are generated using an electrospray process by setting the ESI emitter and the DIMS housing to 3.5 kV and to the ground, respectively. A custom flared glass transfer capillary, which has been shown to improve ion transmission [29], has been used. The position of the electrospray needle is adjusted in order to optimize the ion signal.

The key feature of the DIMS assembly is the set of two parallel plates with dimensions 0.7 × 6 × 20 mm for gap height, width, and length, respectively. Electrosprayed ions are transported by a carrier gas stream at atmospheric pressure between these two electrodes. For this purpose, the desolvation gas which is already implemented in the source region of the tandem mass spectrometer is partially redirected through the outer housing of the DIMS assembly. It thus serves as an ion carrier gas as well as for ion desolvation. Its temperature and flow rate are set using the Bruker control software at 220 °C and 3.5 L min^{-1}, respectively. Modifier gases can be introduced in the N_2 flow in a controlled way using a NanoHPLC (LC-20AD nano, Shimadzu, Kyoto, Japan). The liquid flow rate of the modifier is set to 0.5 μL min^{-1}.

Space separation using the DIMS device is obtained using a bisinusoidal waveform. DIMS peak capacity and resolution strongly depend on the dispersion voltage (DV), which corresponds to the $V_{0\text{-max}}$ of the waveform. The maximum DV value used is 1.8 kV, which corresponds to an electric field of ~ 2.6 10^6 V m^{-1}. A dc offset, referred to as compensation voltage (CV), is applied to one of the electrodes allowing for the transmission of ions of interest through the DIMS device based on their differential ion mobility. DIMS-filtered ions are then transmitted through the capillary to the ion trap where they are accumulated and can be subjected to MS/MS sequences. DIMS spectra, corresponding to the ion count as a function of CV value, are recorded using the abovementioned LabView program. It ensures the synchronization of the scan of the CV mobility parameter with the Bruker acquisition software under chromatogram mode. The centroid of each peak (CV_m) and its full width at half maximum (w_{FWHM}) are derived from Gaussian fits of the experimental DIMS spectra using matlab (R2016b v9.1.0441655, MathWorks). Uncertainties on the CV_m value is on the order of magnitude of the bin width of the DIMS spectra, i.e., 0.1 V. Peak-to-peak resolution (R_{pp}) provides an evaluation of the separation of a pair of peaks. It is derived using Eq. 1. An R_{pp} value greater than 1.5 corresponds to a baseline separation of the two peaks.

$$R_{pp} = \frac{1.178 \times \left|\langle CV\rangle_2 - \langle CV\rangle_1\right|}{w_{FWHM,2} + w_{FWHM,1}} \quad (1)$$

Infrared activation is performed using the tunable mid-infrared (900–1900 cm^{-1}) radiation produced by the free-electron laser (FEL) of the Centre Laser Infrarouge d'Orsay (CLIO) [30]. A hole (0.7 mm diameter) was drilled in the ion trap ring electrode of the quadrupole ion trap allowing for IR irradiation of the trapped ions. The laser band width is 25 cm^{-1}. More details on the experimental setup can be found elsewhere [25]. Two types of experiments combining DIMS selection and IR activation were performed (Eqs. 2 and 3). In the two cases, MS/MS spectra are recorded using the Bruker acquisition software under chromatogram mode, which is synchronized with the scan of the IR wavenumber $\tilde{\nu}$ (Eq. 2) or the scan of the CV parameter (Eq. 3). IR spectra in the 900–1900 cm^{-1} range of DIMS- and mass-selected *m/z* 90 were recorded as described in Eq. 2. The CV voltage was set to a value corresponding to the maximum transmission of the ions of interest (CV_m). The *m/z* 90 ions were mass-selected and accumulated and then irradiated at a given IR wavenumber $\tilde{\nu}$ with a step size of 3 cm^{-1}. Typical irradiation time for these experiments is 200 ms. The second type of DIMS-MS/MS(IRMPD) experiments consists in recording DIMS spectra at fixed IR wavenumber. For each CV

value scanned by step size of 0.1 V, and following the accumulation of the DIMS- and mass-selection, *m/z* 90 ions were irradiated by the IR laser beam. A long irradiation time (500 ms) is used in order to insure significant or even complete depletion of the undesired isomeric ions.

$$\mathrm{DIMS(Fixed\ CV)} \rightarrow {}^{m}/_{z}\ 90\ \mathrm{accumulation\&selection} \rightarrow \mathrm{IR\ irradiation}\ \left(\mathrm{Scanned}\ \tilde{\nu}\right) \quad (2)$$

$$\mathrm{DIMS(Scanned\ CV)} \rightarrow {}^{m}/_{z}\ 90\ \mathrm{accumulation\&selection} \rightarrow \mathrm{IR\ irradiation}\ \left(\mathrm{Fixed}\ \tilde{\nu}\right) \quad (3)$$

Calculated IR absorption spectra of protonated sarcosine, α-alanine, and β-alanine provide a guide for selecting IR signature of each isomer to be used for selective fragmentation of specific isomers. Hybrid density function calculations were carried out with the Gaussian package of programs [31] at the B3LYP/6-311+G** level of theory. Stationary points on the potential energy surface associated with the three protonated isomers have been characterized at this level of theory. Harmonic frequencies of the lowest energy isomers have been scaled by 0.98.

Results and Discussion Section

Differential ion mobility analysis has been carried out with dispersion voltage values ranging from 0.6 to 1.8 kV. No significant differential mobility effect could be observed below 0.6 kV, and dispersion voltages higher than 1.8 kV could lead to electric discharges. For each individual amino acid, DIMS dispersion plots, i.e., the evolution of the CV_m as a function of the DV values, are recorded (Fig. 1). Data recorded with N_2 as a carrier gas is given in solid lines, and those recorded with the addition of methanol as a carrier gas modifier are given in dotted lines. The DIMS spectra recorded at a DV value of 1.8 kV without and with modifier are given in Fig. 2a, b, respectively. For sarcosine uncertainties on CV_m and w_{FWHM}, values are equal to 0.1 V and around 0.05 V, respectively. These values are calculated using the standard deviation over several experiments.

Using only N_2 as a carrier gas, α- and β-alanine cannot be separated, regardless of the dispersion voltage used. These two isomers are however well separated from sarcosine, even at low DV values (Fig. 1). Although similar results have been reported using low electric field ion mobility spectrometry [20, 22], only partial resolution of sarcosine had been achieved. In the present case, a baseline resolution is obtained at 1.8 kV (Fig. 2a), and the corresponding R_{pp} value with α- and β-alanine is 4.9 and 4.2, respectively. As generally observed, the separation capability increases with the dispersion voltage, at the cost of a loss of ion signal. For example, the sarcosine peak is already baseline resolved ($R_{pp} \geq 1.5$) for DV values as low as 1.2 kV, where the ion signal is typically four times greater than at 1.8 kV.

DIMS resolution can also be improved by adding a gas modifier in the N_2 gas flow. The effect of buffer gas modifiers, such as alcohol or other polar and/or proton-acceptor molecules, in ion mobility spectrometry has been already studied in detail [32–34]. The evolution of CV_m as a function of DV, as shown in Fig. 1, is generally assumed to be closely related to the interaction of the ions with the carrier gas, and clustering and declustering may occur at low and high voltage, respectively [32, 34, 35]. The evolution of each CV_m(DV) curve directly reflects the evolution of K, the mobility, as a function of E, the electric field strength, which is commonly expressed as $K=K_0*(1+\alpha(E)*E)$ where K_0 is the mobility constant at low field value and $\alpha(E)$ is the so-called alpha function, which is equal to zero up to an electric field value of the order of 10^4 V m^{-1}.

Three types of DIMS dispersion voltage plots have been observed, each one being associated to a specific $\alpha(E)$ type of function. The three corresponding ion types are termed A, B, and C type ions [35]. Considering the observed CV_m(DV) displayed in Fig. 1, the three present ions behave like A type ions, for which ion-molecule clustering and declustering take place.

Upon addition of methanol, as expected, a negative shift of the CV_m for the three isomers is observed (Fig. 1). At the maximum DV value (1.8 kV), β-alanine is more shifted towards negative values (from − 11 to − 19.7 V) than α-alanine (from − 10.9 to − 18.2 V). As a result, α- and β-alanine are nearly baseline resolved at DV = 1.8 kV (Fig. 2b). The CV_m

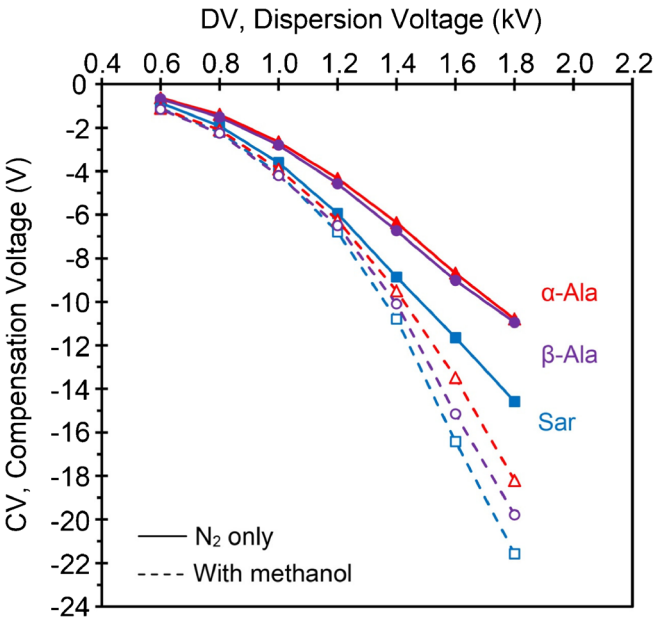

Figure 1. DIMS dispersion plots of the three isomers of *m/z* 90 ions: α-alanine (α-Ala, red triangles), β-alanine (β-Ala, purple circles), and sarcosine (Sar, light blue squares). Data recorded with N_2 only as a carrier gas are given in solid lines, and those recorded with the addition of methanol as a modifier are given in dotted lines. The temperature and N_2 flow rate are set using the Bruker control software at 220 °C and 3.5 L min^{-1}. The methanol liquid flow rate of the modifier is set to 0.5 μL min^{-1}

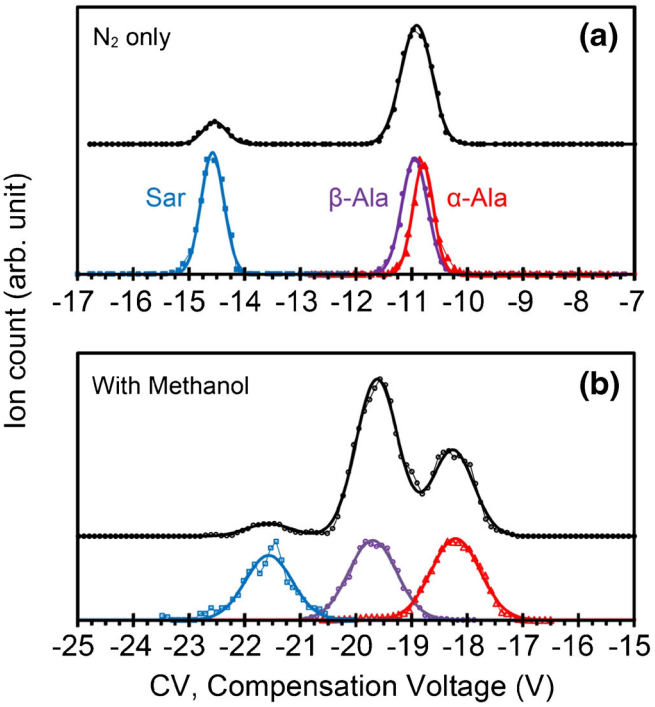

Figure 2. DIMS spectra of three isomers of *m/z* 90 ions: α-alanine (α-Ala, red triangles), β-alanine (β-Ala, purple circles), and sarcosine (Sar, light blue squares). Data were recorded with N_2 only as a carrier gas (a) and with the addition of methanol as a modifier (b). In each panel, the DIMS spectrum of an equimolar mixture of the three isomers is also given (black circles). All individual spectra are normalized to the maximum

value of sarcosine is also shifted from − 14.4 to − 21.6 V upon addition of methanol. Note that a relatively low flow rate (0.5 μL min^{-1}) has been used for introducing methanol into the N_2 carrier gas. The resolution was found to be sensitive to the methanol flow rate, but at the expense of the ion count. The average peak width increases with the addition of the modifier gas (~ 0.50 and 0.65 V without and with methanol as modifier, respectively). As a result, the corresponding R_{pp} value between sarcosine and α-alanine at DV = 1.8 kV decreases from 4.9 to 3.3 upon addition of methanol.

The structure-mobility relationship under high electric field and thus DIMS conditions is not as straightforward as under low electric field conditions. In this context, studies on the effect of buffer gas modifier such as alcohol or other polar and/or proton-acceptor molecules in ion mobility spectrometry provide interesting trends [32–34]. Under low electric field conditions, a decrease of most ion mobilities has been observed [33]. In the context of DIMS, a decrease of the CV_m value has been generally observed upon addition of a polar gas modifier in N_2 carrier gas [36]. Systematic studies of the CV_m(DV) provide evidence for correlation between ion structure and CV_m shifts. More precisely, not only charge site [36] but also steric [37] hindrance can affect the ion-molecule interaction.

Intramolecular ionic hydrogen bond(s) associated to the charge solvation, which is the driving force for conformational structuring in the gas phase, are characteristic of structures of isolated protonated amino acids. Structure of these systems has been the subject of numerous studies since the pioneering work on their fragmentation patterns under low energy collisions [38–40]. Except for amino acids carrying a basic side chain, protonation occurs on the amino group, and hydrogen bonds between the ammonium group and one or more basic sites are formed, as shown in the cases of protonated glycine [41–43], for example.

In the present case, an intramolecular bridge should be formed between an ammonium NH^+ donor and the carboxylic C=O group. The corresponding optimized structures of the three protonated amino acids are shown in Fig. 3. As can be seen in this figure, a five-membered ring is formed in the case of sarcosine and α-alanine, while a six-membered ring is formed in the case of β-alanine. As observed for other systems, this intramolecular hydrogen bond could potentially prevent strong interaction with the solvent and thus from cluster-declustering phenomena [44]. It is interesting to note that the CV_m shift is similar (− 7.2 V) for protonated sarcosine and α-alanine, which both display a five-membered ring hydrogen bond.

Infrared spectroscopy integrated to tandem mass spectrometry provides an excellent means for probing the structural features of mass-selected ions [26]. IRMPD spectra of the three protonated *m/z* 90 isomers have been recorded (Fig. S1). In this figure, experimental IRMPD spectra are compared to the calculated IR absorption spectra predicted for the structures shown in Fig. 3. A band assignment is proposed in Table S1. The three IRMPD spectra are dominated by three types of bands: the carboxylic COH bend near 1150–1200 cm^{-1}, ammonium deformations near 1350–1450 cm^{-1}, and the carboxylic C=O stretch near 1700–1800 cm^{-1}. In addition, only in the cases of α- and β-alanine, an ammonium rocking band is also observed near 1050–1100 cm^{-1}.

Overall, a good match is observed between experimental and predicted spectra for each protonated isomer which supports hydrogen bonding bridge structures shown in Fig. 3. In particular, the position of the carboxylic C=O stretching band is consistent with the calculated IR absorption spectra predicted for the cyclic structures shown in Fig. 3. Therefore, a correlation between the red-shift of the carbonyl C=O stretch and the size of the hydrogen bond cycle is observed. This shift is more pronounced in the case of β-alanine for which the intramolecular charge solvation leads to the formation of a six-membered ring (Fig. S1). The CO stretching band is predicted at 1722 cm^{-1}, i.e., significantly more red-shifted than in the cases of α-alanine (1770 cm^{-1}) and sarcosine (1780 cm^{-1}) whose structures are characterized by a five-membered ring. It thus seems that as found for small protonated peptides [45] and their fragments [46], the C=O stretching region is highly structurally diagnostic.

In the context of this study, a special attention shall be paid to isomer-specific infrared features such as the C=O stretching bands which could be exploited for identifying an

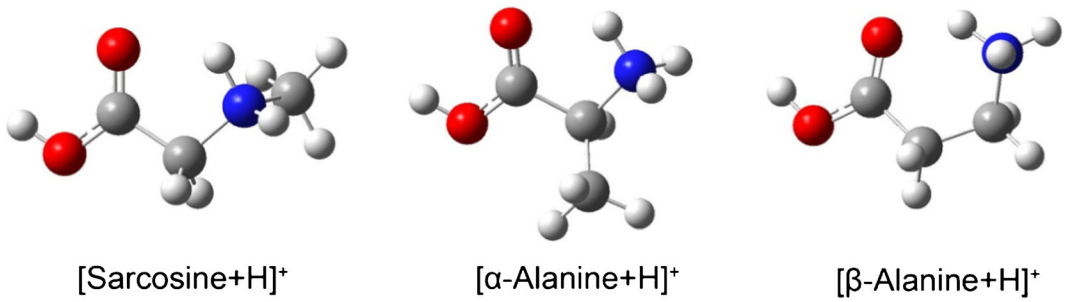

Figure 3. Optimized structures of the three protonated isomers

isomer through specific isomer fragmentation via IRMPD at selected wavenumbers. Based on both predicted and experimental IR spectra (Fig. S1), selective fragmentation of protonated sarcosine could be expected near 1570 cm^{-1}, since the two other isomers have less intense IR bands centered at slightly higher wavenumbers (> 1595 cm^{-1}). Conversely, when irradiating a mixture of the three isomers at ~ 1080 cm^{-1}, i.e., on resonance with a common IR band of both protonated α- and β-alanine, selective or even specific fragmentation could be expected since protonated sarcosine does not present any IR feature between 1000 and 1115 cm^{-1}.

DIMS-MS/MS(IRMPD) spectra shown in Fig. 4 were recording as described in Eq. 3. Following the DIMS selection, MS^2 spectra were recorded where mass-selected *m/z* 90 ions were irradiated by the IR laser beam at a fixed wavenumber. Experiments were performed at different wavenumbers, and the best results were obtained at 1075, 1720, and 1810 cm^{-1}, as illustrated in Fig. 4. The DIMS spectrum reported in Fig. 4a has been recorded with the IR laser off. As discussed above (Fig. 2), using only N_2 as a carrier gas without modifier, α- and β-alanine are separately observed at − 10.9 and − 11.1 V, respectively. The DIMS spectrum of the three-isomer mixture shows a broad peak is observed near − 11.1 V (Fig. 4a), while the sarcosine peak is observed at − 14.5 V.

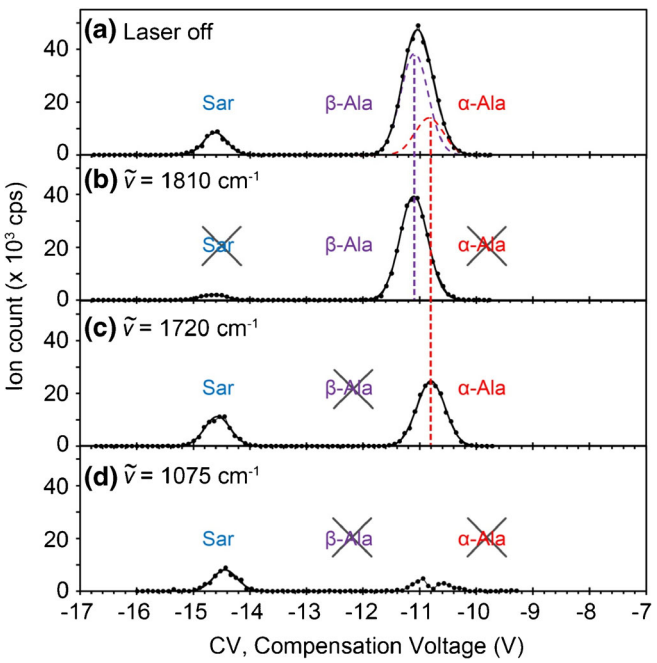

Figure 4. DIMS-MS/MS(IRMPD) spectra of an equimolar mixture of three *m/z* 90 isomers associated with an MS^2 sequence where DIMS- and mass-selected ions were irradiated at selected wavenumbers. Laser off (a), $\tilde{\nu}$ = 1810 cm^{-1} (b), $\tilde{\nu}$ = 1720 cm^{-1} (c), and $\tilde{\nu}$ = 1075 cm^{-1} (d). In each panel, ion counts for the parent (*m/z* 90) are given. Data were recorded with N_2 only as a carrier

Selective isomer fragmentation of DIMS- and mass-selected *m/z* 90 ions was performed exploiting the sensitivity of C=O stretching mode with respect to the size of the hydrogen bond cycle. When the IR wavenumber is set to 1720 cm^{-1}, i.e., on resonance with the C=O stretch of β-alanine, selective fragmentation of this isomer is observed. As shown in Fig. 4c, the sarcosine peak is unchanged, and a narrow peak is observed centered at − 10.9 V corresponding to α-alanine. Conversely, specific fragmentation of protonated sarcosine and α-alanine is observed upon irradiation at 1810 cm^{-1}. Only one narrow peak centered at − 11.1 V corresponding to β-alanine can be seen in the resulting DIMS spectrum shown in Fig. 4b.

The peak assignment in the − 12 to − 10 V region (Fig. 4a–c) is fully consistent with Gaussian fits of the three DIMS spectra. Gaussian fit of each of narrow features in panels b and c led to two similar width (~ 0.5 V), and the CV_m values were found to be − 10.9 and − 11.1 V, respectively, i.e., equal to the CV_m values found for the individual DIMS spectra of α- and β-alanine, respectively. Using these fitted parameters, and only varying the relative amount of α- and β-alanine, a two-Gaussian fit of the broad peak observed centered at − 11.1 V (Fig. 3a) could be well fitted ($R^2 = 0.9981$).

Monitoring the fragmentation patterns, as performed with an MRM approach, at the different wavenumbers offers additional information. This is illustrated in Fig. 5 where DIMS-MS/MS(IRMPD) spectra of both parents and fragments ions are shown. The different MS^2(CID) fragmentation patterns of protonated α- and β-alanine, leading to *m/z* 44 and 72, respectively, can also be exploited for assigning the two components of the DIMS peak at − 11.1 V, as illustrated in Fig. 5b, c. The specific character of the IR activation, however, allows for the selective fragmentation of one or the other isomer, and isomer-specific MRM can be performed.

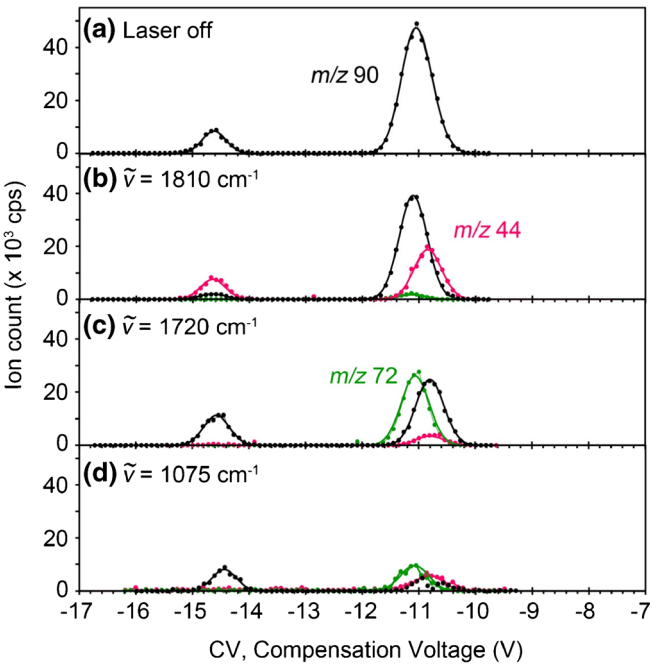

Figure 5. DIMS-MS/MS(IRMPD) spectra of an equimolar mixture of three *m/z* 90 isomers associated with an MS^2 sequence where DIMS- and mass-selected ions were irradiated at selected wavenumbers. Laser off (a), $\tilde{\nu}$ = 1810 cm^{-1} (b), $\tilde{\nu}$ = 1720 cm^{-1} (c), and $\tilde{\nu}$ = 1075 cm^{-1} (d). In each panel, ion counts for the parent (*m/z* 90) and fragment ions (*m/z* 44 and 72) are given. Data were recorded with N_2 only as a carrier

Other DIMS-MS^2(IRMPD) spectra have been recorded with the laser tuned at other wavenumber values. As discussed above, selective fragmentation of protonated sarcosine could be expected near 1570 cm^{-1}, since the predicted IR absorbance of this isomer is larger than that of the two other isomers. Unfortunately, poor selectivity was achieved, probably due to the fact that the relatively large bandwidth of the laser bandwidth (20–25 cm^{-1}). Conversely, however, almost full depletion of α- and β-alanine signals could be observed at 1075 cm^{-1} (Fig. 4d) while the DIMS peak of sarcosine remains unchanged. At this IR wavenumber, protonated α- and β-alanine have a characteristic band of the ammonium rock, while the IR absorbance is zero for protonated sarcosine. As a result, specific fragmentation of protonated α- and β-alanine could be achieved at 1075 cm^{-1}, thus allowing for the unambiguous assignment of the DIMS peak of protonated sarcosine even without referring to reference date for the pure standards (colored tracks in Fig. 2).

The advantage of IR activation of collisional action is particularly interesting when the three protonated isomers are irradiated at 1075 cm^{-1}. As can be seen in Fig. 5d, the *m/z* 44 and 72 fragment ions are observed with maximum intensities at CV values of − 10.9 and − 11.1 V, respectively. These fragmentations are the signature of the α- and β-alanine isomers. The isomer selectivity of the IR activation is also evidenced by the fact that no fragmentation is observed for CV values close to − 14.5 V, corresponding to the protonated sarcosine.

Conclusion

A simple method for the rapid separation and identification of sarcosine and α- and β-alanine isomers is reported. An efficient separation of these isomers can be achieved using a DIMS device interfaced with the tandem mass spectrometer, especially when methanol is added in the dinitrogen carrier gas. DIMS peak identification using MS/MS, where DIMS- and mass-selected ions are selectively activated by resonant absorption of IR light, has been demonstrated. DIMS-MS/MS(IRMPD) spectra recorded at different fixed wavenumber values illustrate the potential of the methods. Specific depletion of α- and β-alanine isomers can be achieved, and the resulting DIMS-MS/MS(IRMPD) spectra only display the sarcosine peak. The proposed method is also particularly useful for resolving overlapping DIMS peaks. The different components can be selectively depleted by tuning the IR wavenumber on isomer-specific absorption bands.

Chromatographic and/or mobility separation associated with identification with standard MS/MS methods can be routinely used for small molecule mixtures, where identification and quantification relies on MRM methods. However, identification of isomers with the same MS/MS ion transitions, such as sarcosine and α-alanine, remains a difficult task. It is shown here that MS/MS-based methods with isomer-specific ion activation can overcome these limits. IR activation is particularly well-suited for the selective activation of constitutional isomers, which can be separated by liquid chromatography [47] or by an ion mobility-based technique. As illustrated here, comparison of DIMS-MS/MS(IRMPD) spectra recorded at different selected laser wavelengths can allow for a fast identification of such isomers.

Acknowledgments

We are thankful to the three reviewers for their constructive comments and suggestions.

Funding This work is supported by a public grant from the "Laboratoire d'Excellence Physics Atom Light Mater" (LabEx PALM) overseen by the French National Research Agency (ANR) as part of the "Investissements d'Avenir" program (reference: ANR-10-LABX-0039). Financial support from the Centre National de la Recherche Scientifique (CNRS) is gratefully acknowledged.

References

1. Siminska, E., Koba, M.: Amino acid profiling as a method of discovering biomarkers for early diagnosis of cancer. Amino Acids. **48**, 1339–1345 (2016)
2. Hasim, A., Aili, A.X.Z., Maimaiti, A., Mamtimin, B., Abudula, A., Upur, H.: Plasma-free amino acid profiling of cervical cancer and cervical intraepithelial neoplasia patients and its application for early detection. Mol. Biol. Rep. **40**, 5853–5859 (2013)
3. Miyagi, Y., Higashiyama, M., Gochi, A., Akaike, M., Ishikawa, T., Miura, T., Saruki, N., Bando, E., Kimura, H., Imamura, F., Moriyama, M., Ikeda, I., Chiba, A., Oshita, F., Imaizumi, A., Yamamoto, H.,

Miyano, H., Horimoto, K., Tochikubo, O., Mitsushima, T., Yamakado, M., Okamoto, N.: Plasma free amino acid profiling of five types of cancer patients and its application for early detection. PLoS One. **6**, e24143 (2011)
4. Maeda, J., Higashiyama, M., Imaizumi, A., Nakayama, T., Yamamoto, H., Daimon, T., Yamakado, M., Imamura, F., Kodama, K.: Possibility of multivariate function composed of plasma amino acid profiles as a novel screening index for non-small cell lung cancer: a case control study. BMC Cancer. **10**, 690 (2010)
5. Kim, H.J., Jang, S.H., Ryu, J.S., Lee, J.E., Kim, Y.C., Lee, M.K., Jang, T.W., Lee, S.Y., Nakamura, H., Nishikata, N., Mori, M., Noguchi, Y., Miyano, H., Lee, K.Y.: The performance of a novel amino acid multivariate index for detecting lung cancer: a case control study in Korea. Lung Cancer. **90**, 522–527 (2015)
6. Leichtle, A.B., Nuoffer, J.M., Ceglarek, U., Kase, J., Conrad, T., Witzigmann, H., Thiery, J., Fiedler, G.M.: Serum amino acid profiles and their alterations in colorectal cancer. Metabolomics. **8**, 643–653 (2012)
7. Dietzen, D.J., Weindel, A.L., Carayannopoulos, M.O., Landt, M., Normansell, E.T., Reimschisel, T.E., Smith, C.H.: Rapid comprehensive amino acid analysis by liquid chromatography/tandem mass spectrometry: comparison to cation exchange with post-column ninhydrin detection. Rapid Commun. Mass Spectrom. **22**, 3481–3488 (2008)
8. Prinsen, H., Schiebergen-Bronkhorst, B.G.M., Roeleveld, M.W., Jans, J.J.M., de Sain-van der Velden, M.G.M., Visser, G., van Hasselt, P.M., Verhoeven-Duif, N.M.: Rapid quantification of underivatized amino acids in plasma by hydrophilic interaction liquid chromatography (HILIC) coupled with tandem mass-spectrometry. J. Inherit. Metab. Dis. **39**, 651–660 (2016)
9. Khamis, M.M., Adamko, D.J., El-Aneed, A.: Mass spectrometric based approaches in urine metabolomics and biomarker discovery. Mass Spectrom. Rev. **36**, 115–134 (2017)
10. Dunn, W.B., Broadhurst, D., Begley, P., Zelena, E., Francis-McIntyre, S., Anderson, N., Brown, M., Knowles, J.D., Halsall, A., Haselden, J.N., Nicholls, A.W., Wilson, I.D., Kell, D.B., Goodacre, R., Human Serum Metabolome (HUSERMET) Consortium: Procedures for large-scale metabolic profiling of serum and plasma using gas chromatography and liquid chromatography coupled to mass spectrometry. Nat. Protoc. **6**, 1060–1083 (2011)
11. Martin-Girardeau, A., Renou-Gonnord, M.F.: Optimization of a capillary electrophoresis-electrospray mass spectrometry method for the quantitation of the 20 natural amino acids in childrens blood. J. Chromatogr. B. **742**, 163–171 (2000)
12. Soga, T., Heiger, D.N.: Amino acid analysis by capillary electrophoresis electrospray ionization mass spectrometry. Anal. Chem. **72**, 1236–1241 (2000)
13. Lapthorn, C., Pullen, F., Chowdhry, B.Z.: Ion mobility spectrometry-mass spectrometry (IMS-MS) of small molecules: separating and assigning structures to ions. Mass Spectrom. Rev. **32**, 43–71 (2013)
14. Paglia, G., Astarita, G.: Metabolomics and lipidomics using traveling-wave ion mobility mass spectrometry. Nat. Protoc. **12**, 797–813 (2017)
15. Fu, Y.L., Xia, Y.Q., Flarakos, J., Tse, F.L.S., Miller, J.D., Jones, E.B., Li, W.K.: Differential mobility spectrometry coupled with multiple ion monitoring in regulated LC-MS/MS bioanalysis of a therapeutic cyclic peptide in human plasma. Anal. Chem. **88**, 3655–3661 (2016)
16. Dwivedi, P., Schultz, A.J., Hill, H.H.: Metabolic profiling of human blood by high-resolution ion mobility mass spectrometry (IM-MS). Int. J. Mass Spectrom. **298**, 78–90 (2010)
17. Schneider, B.B., Nazarov, E.G., Londry, F., Vouros, P., Covey, T.R.: Differential mobility spectrometry/mass spectrometry history, theory, design optimization, simulations, and applications. Mass Spectrom. Rev. **35**, 687–737 (2016)
18. Sreekumar, A., Poisson, L.M., Rajendiran, T.M., Khan, A.P., Cao, Q., Yu, J.D., Laxman, B., Mehra, R., Lonigro, R.J., Li, Y., Nyati, M.K., Ahsan, A., Kalyana-Sundaram, S., Han, B., Cao, X.H., Byun, J., Omenn, G.S., Ghosh, D., Pennathur, S., Alexander, D.C., Berger, A., Shuster, J.R., Wei, J.T., Varambally, S., Beecher, C., Chinnaiyan, A.M.: Metabolomic profiles delineate potential role for sarcosine in prostate cancer progression. Nature. **457**, 910–914 (2009)
19. Heger, Z., Rodrigo, M.A.M., Michalek, P., Polanska, H., Masarik, M., Vit, V., Plevova, M., Pacik, D., Eckschlager, T., Stiborova, M., Adam, V.: Sarcosine up-regulates expression of genes involved in cell cycle progression of metastatic models of prostate cancer. PLoS One. **11**, (2016)
20. Mirmahdieh, S., Khayamian, T.: Separation of sarcosine and L-alanine isomers using corona discharge ion mobility spectrometry. J. Anal. Chem. **69**, 513–518 (2014)
21. Johnson, P.V., Kim, H.I., Beegle, L.W., Kanik, I.: Electrospray ionization ion mobility spectrometry of amino acids: ion mobilities and a mass-mobility correlation. J. Phys. Chem. A. **108**, 5785–5792 (2004)
22. Martinez-Lozano, P., Rus, J.: Separation of isomers L-alanine and sarcosine in urine by electrospray ionization and tandem differential mobility analysis-mass spectrometry. J. Am. Soc. Mass Spectrom. **21**, 1129–1132 (2010)
23. Beegle, L.W., Kanik, I., Matz, L., Hill, H.H.: Electrospray ionization nigh-resolution ion mobility spectrometry for the detection of organic compounds, 1. Amino acids. Analytical Chemistry. **73**, 3028–3034 (2001)
24. Barnett, D.A., Ells, B., Guevremont, R., Purves, R.W.: Separation of leucine and isoleucine by electrospray ionization-high field asymmetric waveform ion mobility spectrometry-mass spectrometry. J. Am. Soc. Mass Spectrom. **10**, 1279–1284 (1999)
25. Mac Aleese, L., Simon, A., McMahon, T.B., Ortega, J.M., Scuderi, D., Lemaire, J., Maitre, P.: Mid-IR spectroscopy of protonated leucine methyl ester performed with an FTICR or a Paul type ion-trap. Int. J. Mass Spectrom. **249**, 14–20 (2006)
26. MacAleese, L., Maitre, P.: Infrared spectroscopy of organometallic ions in the gas phase: from model to real world complexes. Mass Spectrom. Rev. **26**, 583–605 (2007)
27. Isenberg, S.L., Armistead, P.M., Glish, G.L.: Optimization of peptide separations by differential ion mobility spectrometry. J. Am. Soc. Mass Spectrom. **25**, 1592–1599 (2014)
28. Hernandez, O., Isenberg, S., Steinmetz, V., Glish, G.L., Maitre, P.: Probing mobility-selected saccharide isomers: selective ion-molecule reactions and wavelength-specific IR activation. J. Phys. Chem. A. **119**, 6057–6064 (2015)
29. Campbell, M.T., Glish, G.L.: Increased ion transmission for differential ion mobility combined with mass spectrometry by implementation of a flared inlet capillary. J. Am. Soc. Mass Spectrom. **28**, 119–124 (2017)
30. Prazeres, R., Glotin, F., Insa, C., Jaroszynski, D.A., Ortega, J.M.: Two-colour operation of a free-electron laser and applications in the mid-infrared. European Physical Journal D: Atomic, Molecular and Optical Physics. **3**, 87–93 (1998)
31. Frisch, M.J., Trucks, G.W., Schlegel, H.B., Scuseria, G.E., Robb, M.A., Cheeseman, J.R., Scalmani, G., Barone, V., Mennucci, B., Petersson, G.A., Nakatsuji, H., Caricato, M., Li, X., Hratchian, H.P., Izmaylov, A.F., Bloino, J., Zheng, G., Sonnenberg, J.L., Hada, M., Ehara, M., Toyota, K., Fukuda, R., Hasegawa, J., Ishida, M., Nakajima, T., Honda, Y., Kitao, O., Nakai, H., Vreven, T., Montgomery Jr., J.A., Peralta, J.E., Ogliaro, F., Bearpark, M.J., Heyd, J., Brothers, E.N., Kudin, K.N., Staroverov, V.N., Kobayashi, R., Normand, J., Raghavachari, K., Rendell, A.P., Burant, J.C., Iyengar, S.S., Tomasi, J., Cossi, M., Rega, N., Millam, N.J., Klene, M., Knox, J.E., Cross, J.B., Bakken, V., Adamo, C., Jaramillo, J., Gomperts, R., Stratmann, R.E., Yazyev, O., Austin, A.J., Cammi, R., Pomelli, C., Ochterski, J.W., Martin, R.L., Morokuma, K., Zakrzewski, V.G., Voth, G.A., Salvador, P., Dannenberg, J.J., Dapprich, S., Daniels, A.D., Farkas, Foresman, J.B., Ortiz, J.V., Cioslowski, J., Fox, D.J.: Gaussian 09. Gaussian, Inc., Wallingford (2009)
32. Eiceman, G.A., Krylov, E.V., Nazarov, E.G., Miller, R.A.: Separation of ions from explosives in differential mobility spectrometry by vapor-modified drift gas. Anal. Chem. **76**, 4937–4944 (2004)
33. Fernandez-Maestre, R., Wu, C., Hill, H.H.: Buffer gas modifiers effect resolution in ion mobility spectrometry through selective ion-molecule clustering reactions. Rapid Commun. Mass Spectrom. **26**, 2211–2223 (2012)
34. Krylova, N., Krylov, E., Eiceman, G.A., Stone, J.A.: Effect of moisture on the field dependence of mobility for gas-phase ions of organophosphorus compounds at atmospheric pressure with field asymmetric ion mobility spectrometry. J. Phys. Chem. A. **107**, 3648–3654 (2003)
35. Guevremont, R., Purves, R.W.: High field asymmetric waveform ion mobility spectrometry-mass spectrometry: an investigation of leucine enkephalin ions produced by electrospray ionization. J. Am. Soc. Mass Spectrom. **10**, 492–501 (1999)
36. Campbell, J.L., Zhu, M., Hopkins, W.S.: Ion-molecule clustering in differential mobility spectrometry: lessons learned from tetraalkylammonium cations and their isomers. J. Am. Soc. Mass Spectrom. **25**, 1583–1591 (2014)

37. Liu, C., Le Blanc, J.C.Y., Shields, J., Janiszewski, J.S., Ieritano, C., Ye, G.F., Hawes, G.F., Hopkins, W.S., Campbell, J.L.: Using differential mobility spectrometry to measure ion solvation: an examination of the roles of solvents and ionic structures in separating quinoline-based drugs. Analyst. **14**, 6897–6903 (2015)
38. Bouchonnet, S., Hoppilliard, Y.: Proton and sodium-ion affinities of glycine and its sodium-salt in the gas-phase—ab initio calculations. Org. Mass Spectrom. **27**, 71–76 (1992)
39. Jensen, F.: Structure and stability of complexes of glycine and glycine methyl analogs with H+, Li+, and Na+. J. Am. Chem. Soc. **114**, 9533–9537 (1992)
40. Dookeran, N.N., Yalcin, T., Harrison, A.G.: Fragmentation reactions of protonated alpha-amino acids. J. Mass Spectrom. **31**, 500–508 (1996)
41. O'Hair, R.A.J., Broughton, P.S., Styles, M.L., Frink, B.T., Hadad, C.M.: The fragmentation pathways of protonated glycine: a computational study. J. Am. Soc. Mass Spectrom. **11**, 687–696 (2000)
42. Armentrout, P.B., Heaton, A.L., Ye, S.J.: Thermodynamics and mechanisms for decomposition of protonated glycine and its protonated dimer. J. Phys. Chem. A. **115**, 11144–11155 (2011)
43. Meroueh, S.O., Wang, Y.F., Hase, W.L.: Direct dynamics simulations of collision- and surface-induced dissociation of N-protonated glycine. Shattering fragmentation. Journal of Physical Chemistry A. **106**, 9983–9992 (2002)
44. Lintonen, T.P.I., Baker, P.R.S., Suoniemi, M., Ubhi, B.K., Koistinen, K.M., Duchoslav, E., Campbell, J.L., Ekroos, K.: Differential mobility spectrometry-driven shotgun lipidomics. Anal. Chem. **86**, 9662–9669 (2014)
45. Wu, R.H., McMahon, T.B.: Infrared multiple photon dissociation spectroscopy as structural confirmation for $GlyGlyGlyH^+$ and $AlaAlaAlaH^+$ in the gas phase. Evidence for amide oxygen as the protonation site. J. Am. Chem. Soc. **129**, 11312 (2007)
46. Hernandez, O., Paizs, B., Maitre, P.: Rearrangement chemistry of a_n ions probed by IR spectroscopy. Int. J. Mass Spectrom. **377**, 172–178 (2015)
47. Martens, J., Berden, G., van Outersterp, R.E., Kluijtmans, L.A.J., Engelke, U.F., van Karnebeek, C.D.M., Wevers, R.A., Oomens, J.: Molecular identification in metabolomics using infrared ion spectroscopy. Sci. Rep. **7**, 3363 (2017)